Shock and Vibration 9 (2002) 57–66
IOS Press

Wavenumber processing techniques to determine structural intensity and its divergence from optical measurements without leakage effects

Jean-Claude Pascal[a,*], Jing-Fang Li[b] and Xavier Carniel[c]
[a]*Ecole Nationale Supérieure d'Ingénieurs du Mans* (*ENSIM*) *and Institut d'Acoustique et de Mécanique* (*IAM*), *Université du Maine, rue Aristote, 72000 Le Mans, France*
[b]*Visual VibroAcoustics, 51 rue d'Alger, 72000 Le Mans, France*
[c]*Centre Technique des Industries Mécaniques* (*CETIM*), *52 avenue Felix-Louat BP 80067, 60300 Senlis, France*

Abstract: The technique of processing data in the wavenumber domain based on the Spatial Fourier Transform (SFT), is a powerful tool to compute higher-order partial derivatives occurred in the expressions of the structural intensity and its divergence. However, performing directly the SFT usually results in great distortions if a discontinuity occurs in spatial periodicity (leakage effect). The worst thing is that the divergence of a free plate cannot correctly be estimated by existing wavenumber processing such as the STF and zero padding method. In this paper, a new algorithm – mirror processing, is developed. By the use of vibrating velocity measured from the technique of laser scanning vibrometry, the structural intensity, its divergence and the force distribution are evaluated by different techniques of wavenumber processing. It is shown that the distortions caused by leakage effects can be removed by using advanced algorithms.

1. Introduction

The structural intensity has been used to describe the power transferred by elastic waves through mechanical structures. It is different from the modal analysis in the fact that the modal analysis is a representation of the stationary waves of a vibrating system whereas the structural intensity describes energy flow and transfer paths. It has been shown that the information from the analysis of the structural intensity is very important in noise control engineering [1]. The divergence of the structural intensity has been used to identify the power injected and dissipated by external elements such as mechanical excitation, dampers and radiation regions [2].

Based on the theoretical expressions of the structural intensity for a planar plate, which are associated with the calculation of the normal velocity and the spatial derivatives of normal vibrating velocity when only the flexural waves are considered [3,4], two methods were used for determining experimentally the structural intensity, finite difference approximation and the use of Spatial Fourier Transform (SFT). The finite difference approximation was first used in 1969 [3]. A complete formulation for the structural intensity in plate and beam was derived using the finite difference approximation [4]. However a set of sensors are needed. It was shown that thirteen accelerometers were used and thirty-four cross-spectrum measurements [17] or nine accelerometers and twenty cross-spectra [5] were required to determine the complex structural intensity.

*Corresponding author: Prof. Jean-Claude Pascal, Ecole Nationale Supérieure d'Ingénieurs du Mans (ENSIM), Université du Maine, rue Aristote,, 72085 Le Mans CEDEX 09, France. Tel.: +33 2 43 83 39 53; Fax: +33 2 43 83 37 94; E-mail: Jean-Claude.Pascal@univ-lemans.fr.

ISSN 1070-9622/02/$8.00

The accelerometers were mounted on the structure in order to obtain experimentally the complex structural intensity, resulting in errors because of extra loading imposed on the structure. Besides, distortions can be produced by the far-field approximations related to the four sensor techniques [5,6,17]. The divergence of the structural intensity in a planar plate, which can well be used to locate mechanical excitations [2,8], is expressed in terms of higher order partial derivatives [2]. Thirteen points are required to determine the partial derivatives by the use of the standard finite difference approximation. This solution is not usable for experimental procedures.

The limitations caused by finite difference approximation for determination of the structural intensity and divergence can be overcomed by the use of the wavenumber processing technique. The key to this technique is to calculate the spatial derivatives by the Spatial Fourier Transform (SFT). This approach was already associated with the techniques of near-field acoustic holography [2,7] and laser vibrometry measurements [8,9]. Holographic interferometry which makes it possible to obtain the data at high density of points, is necessary for processing in the wavenumber domain [10–12].

However, it is well known that the use of the SFT is often accompanied by large distortions if the signal has discontinuities in the space periodicity (leakage effect). If the SFT is directly used, the results are very sensitive to the boundary conditions. One cannot obtain a good estimation of the spectrum in wavenumber domain. It then results errors in the calculations of the structural intensity and divergence. A method called Regressive Fourier Transform has been proposed to solve this problem [13]. The inverse method can be used to minimize the leakage problem by a better estimation of the wavenumber spectrum, which results in good estimation in partial derivatives. However the algorithm is sometimes hard to be automatically used because of trial-and-error parameters.

The present work focuses on developing new algorithms for processing in wavenumber domain without leakage effects when SFT is performed for calculation of the structural intensity and divergence in a planar plate. In the second section, the formulations of the structural intensity and its divergence are written in terms of the normal velocity in a plate. Meanwhile expression for calculating force distributions is given. The Section 3 shows the application of the optical measurements – holographic interferometry and/or laser vibrometry – in the determination of the normal complex vibrating velocity on the plate. Experimental descriptions for these techniques are made briefly. In the fourth section the new algorithm – mirror processing in wavenumber domain – is described. The use of the new technique for calculation of the derivatives in wavenumber domain is demonstrated. Comparisons are made among the methods such as direct Fourier transform, zero padding and the mirror processing.

Section 5 shows the structural intensity, the divergence and force distributions determined by processing the measured normal velocity in plate in wavenumber domain. It is noted that the mirror algorithm can remove the leakage effects caused by discontinuities in the space periodicity of signals. The new algorithms allow excitation points to be located precisely, whereas the direct use of Fourier transform fails.

2. Formulations of structural intensity and divergence in a plate

The expressions for the structural intensity, its divergence and the exciting force distributions have been given in [1–4,14]. For the sake of completeness, they are recalled in this section. The expressions for calculations by SFT are also written.

2.1. Structural intensity, divergence and force distributions

2.1.1. Flexural waves in plates

Structural intensity in a plate means the energy flow per unit length in a given direction. By expressing the shear forces and bending and twisting moments [1–4], the x- and y-components of the structural intensity are written by (time dependent factor $e^{j\omega t}$ is used),

$$I_x = \frac{B}{2\omega}\mathrm{Im}\left\{\frac{\partial}{\partial x}(\nabla^2 v)v^* - \left(\frac{\partial^2 v}{\partial x^2} + \upsilon\frac{\partial^2 v}{\partial y^2}\right)\frac{\partial v^*}{\partial x} - (1-\upsilon)\frac{\partial^2 v}{\partial x \partial y}\,\frac{\partial v^*}{\partial y}\right\}, \tag{1a}$$

$$I_y = \frac{B}{2\omega}\mathrm{Im}\left\{\frac{\partial}{\partial y}(\nabla^2 v)v^* - \left(\frac{\partial^2 v}{\partial y^2} + \upsilon\frac{\partial^2 v}{\partial x^2}\right)\frac{\partial v^*}{\partial y} - (1-\upsilon)\frac{\partial^2 v}{\partial x \partial y}\,\frac{\partial v^*}{\partial x}\right\}. \tag{1b}$$

with v the normal velocity, v^* the complex conjugate of the normal velocity, $B = Eh^3/12(1-\upsilon^2)$ the bending stiffness. E is Young's modulus, h is the thickness of the plate and υ is Poisson's ratio. The first term in Eqs (1a) and (1b) is the product of the shear force per unit length by velocity v. The second term is the product of the bending moment per unit length by the angular velocity caused by the bending movement. The third term is the product of the twisting moment per unit length by the angular velocity caused by the twist movement. It is demonstrated [2] that Eqs (1a) and (1b) can be written into a more concise form using the 3D operator nabla where $\partial/\partial z \equiv 0$

$$\mathbf{I} = \frac{B}{2\omega}\mathrm{Im}\left\{\nabla(\nabla^2 v)v^* - \nabla^2 v\nabla v^* - \frac{1-\upsilon}{2}\nabla\times\nabla\times(v\nabla v^*)\right\}. \tag{2}$$

The above expressions are results of the Kirchoff plate theory. For one-dimensional intensity, Sander [15] compared the formula using the Euler Bernoulli model with that using the Timoshenko beam model including shear deformation and rotational inertia. Comparisons between power flow from Kirchoff and Mindlin theory are made in [14]. The two expressions are equivalent at low frequencies. The usual condition $\lambda = 6h$ (h is the thickness of the beam) can be used to define the upper limit of validity of these derivations [16].

2.1.2. Injected power

The energy conservation equation for a plate with the damping neglected is written in the form: $\oint_l \mathbf{I}\cdot\hat{\mathbf{n}}dl = \iint_S \nabla\cdot\mathbf{I}dS = 0$, where S is the area of the portion of the plate limited by the closed contour l, through which is determined the flux of vector $\mathbf{I}$ (with $\hat{\mathbf{n}}$ the normal unit vector at contour l). This equation is not equal to zero if an energy flow $w(x,y)$ crosses the surface of the plate. This flow may be produced by mechanical excitation (sources) and local or distributed damping on the structure (sinks : added dissipating elements, or, if applicable, acoustic radiation). The integrated intensity flux on closed contour l corresponds to the power injected (positive) or dissipated (negative) by the external elements

$$\begin{aligned}\oint_l \mathbf{I}(x,y)\cdot\hat{\mathbf{n}}dl &= \iint_S \nabla\cdot\mathbf{I}(x,y)dS \\ &= \iint_S w(x,y)dS \\ &= W.\end{aligned} \tag{3}$$

Equation (3) shows that the divergence of active intensity of the flexural waves in the plate is equal to the surface density of injected (or dissipated) power,

$$\nabla\cdot\mathbf{I}(x,y) = w(x,y). \tag{4}$$

Substituting expression Eq. (2) into Eq. (4) yields [2]

$$\nabla\cdot\mathbf{I} = \frac{B}{2\omega}\mathrm{Im}\left\{(\nabla^4 v)v^*\right\}. \tag{5}$$

The divergence of the structural intensity can be thus determined from the normal vibrating velocity in a plate.

2.1.3. Force distributions

The external forces $F(x,y)$ applied to a plate can also be evaluated from the normal vibrating velocity $v(x,y)$ by the use of the inhomogeneous differential equation of the bending waves in the Kirchoff plates

$$\nabla^4(x,y) - k_B^4(x,y) = j\omega\frac{F(x,y)}{B}, \tag{6}$$

where $k_B^4 = \omega^2[12(1-\upsilon^2)\rho/Eh^2]$ is the bending wavenumber in a plate and B the bending stiffness. It is shown that the force distribution is related not only to the vibrating velocity but also to the double Laplacian operator of it.

By Eqs (2), (5) and (6) it is shown that higher-order partial derivatives of the vibrating velocity $v(x,y)$ with respect to the coordinate x and y should firstly be known in order to obtain the structural intensity, divergence and force distributions. Experimentally, it is impossible to measure all the derivatives because of the limit of the numbers of sensors [5,6,18]. The technique of wavenumber processing can be used to calculate any order derivatives. So it is necessary in the following section to give expressions of the structural intensity, divergence and force distributions in wavenumber space.

2.2. Calculations of the structural intensity, divergence and force in wavenumber space

The principle of calculation in wavenumber domain is the application of the Spatial Fourier Transform (SFT). As an example, when making use of the Cartesian coordinate system, the SFT of the derivatives $\frac{\partial^{m+n}v(x,y)}{\partial^m x\partial^n y}$ is written by [7]

$$\frac{\partial^{m+n}v(x,y)}{\partial^m x\partial^n y} \overset{SFT}{\mapsto} (-jK_x)^m(-jK_y)^n V(K_x,K_y), \tag{7}$$

where $V(K_x, K_y)$ is the Spatial Fourier Transform of $v(x, y)$. K_x and K_y are wavenumbers respectively in $\hat{\mathbf{k}}_\mathbf{x}$ and $\hat{\mathbf{k}}_\mathbf{y}$ directions. The higher-order partial derivative $\frac{\partial^{m+n} v(x,y)}{\partial^m x \partial^n y}$ can be obtained by performing simply the inverse SFT to the right-hand side of Eq. (7). By making use of this method, the structural intensity can be computed by performing the SFT to Eq. (2)

$$\begin{aligned}\mathbf{I}(x,y) = \frac{B}{2\omega}\mathbf{Im}\Big\{ & F^{-1}\left\{j\mathbf{K}^3 V(K_x,K_y)\right\} v^* \\ & -F^{-1}\left\{\mathbf{K}^2 V(K_x,K_y)\right\} \\ & F^{-1}\left\{j\mathbf{K} V^*(K_x,K_y)\right\} \\ & +\frac{1-v}{2}F^{-1}\left\{\mathbf{K}\times\mathbf{K}\times F\left\{v\nabla v^*\right\}\right\}\Big\}\end{aligned} \tag{8}$$

Similarly, from Eq. (5) the divergence of the structural intensity is expressed by

$$\begin{aligned}\nabla\times\mathbf{I} = -\frac{B}{2\omega}\mathrm{Im}\left\{F^{-1}\left\{\mathbf{K}^4 V(K_x,K_y)\right\}\right. \\ \left. F^{-1}\left\{V^*(K_x,K_y)\right\}\right\},\end{aligned} \tag{9}$$

and by Eq. (6) the force distributions can be written in the form,

$$\begin{aligned}F = -j\frac{B}{\omega}\left\{F^{-1}\left\{\mathbf{K}^4 V(K_x,K_y)\right\}\right. \\ \left. -F^{-1}\left\{k_B^4 V(K_x,K_y)\right\}\right\}.\end{aligned} \tag{10}$$

where $\mathbf{K} = K_x\hat{\mathbf{k}}_x + K_y\hat{\mathbf{k}}_y$, F^{-1} represents the inverse SFT. Equations (8)–(10) are three basic expressions used in this paper to calculate the structural intensities, the divergence of the structural intensity in a plate and the force distributions from a normal component of the vibrating velocity.

3. Determinations of complex velocity by optical measurements

Equations (8)–(10) show that the normal component of the complex velocity in a plate suffices for calculations of the structural intensity, the divergence and the force distributions. The optical measurement techniques such as the holographic interferometry [10–12] and laser vibrometry [8,9] have well been applied to measure the vibrating complex velocity (amplitudes and phases) on the plate without contact. This section illustrates how to determine experimentally the complex vibrating velocity using the two optic techniques.

3.1. Holographic interferometry

The experimental procedure depends on the technique of double-exposure and double-reference holography. A hologram is created at the recording time, which can be reconstructed, after processing, to provide a global image of the instantaneous velocity field of the vibrating structure. The production of two such holograms during the same period allows the determination of the amplitude and phase of the vibrational field.

Two exposures at two almost identical instants allow the two vibrational states of the object under examination to be recorded on the same photosensitive sheet. When these are reconstructed using the same coherent light source (continuous laser), the interference fringes observed show the difference in the movement in the two exposures. If each exposure uses its own reference beam, two independent holograms are recorded on the same sheet (see Fig. 1). For the reconstruction, two-reference beams are simultaneously used to produce two holographic images, thereby providing two reconstructed light waves, each of which corresponds to a different state of the object, whose optical phase can be varied using a piezo-electric mirror placed on one of the reference beams used for the reconstruction. A double exposure, double reference recording leads to a time finite difference approximation of the vibrational velocity.

Two double-exposure and double-reference recordings during a period $T = 2\pi/\omega$ allow one to obtain two values for the instantaneous velocity over the whole of the surface illuminated. Details of the processing can be found in [10,11]. The cinehology technique was used for this study. Each double-exposure hologram is sampled at 25 Hz [12]. The method of speckle interferometry was also applied in some experimental measurements [19,23]. As an example, Fig. 2 illustrates the image of the interference patterns corresponding to one double exposure.

3.2. Laser vibrometry technique

For the acquisitions, a scanning vibrometer was used, together with LMS software. It uses an OFV 300 optical head from Polytec, which comprises a single point interferometer with a motor-driven control-focusing device. Two galvo-driven mirrors direct the laser beam horizontally and vertically. It allows one to obtain easily the 1024 (32×32) measurement points with a high resolution on a large frequency range. In

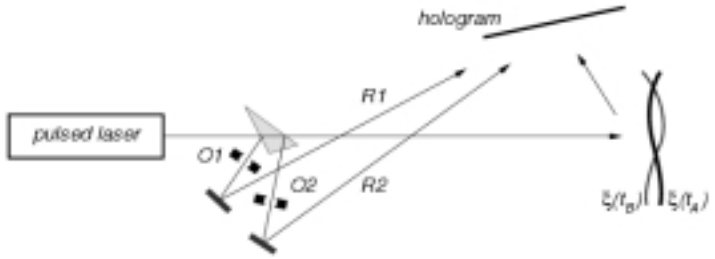

Fig. 1. Recording of a double exposure, double reference hologram. The two reference beams form a slight angle relative to one another: at t_A, reference R1 (shutter O2 closed); at t_B, reference R2 (shutter O1 closed).

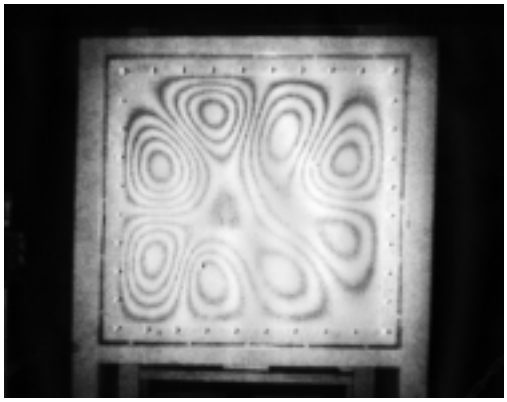

Fig. 2. Image of the interference patterns corresponding to one double exposure at t_A and t_B shown in Fig. 1. The vibrating velocity in the plate at an instant is obtained by processing this image.

Fig. 3 is demonstrated the experimental set-up for measuring the vibrating velocity in the plate by the use of the technique of the scanning laser vibrometry. In this paper the velocity data recorded from this experimental set-up will be processed by in wavenumber domain to obtain the structural intensity, the divergence and the excitation force distributions.

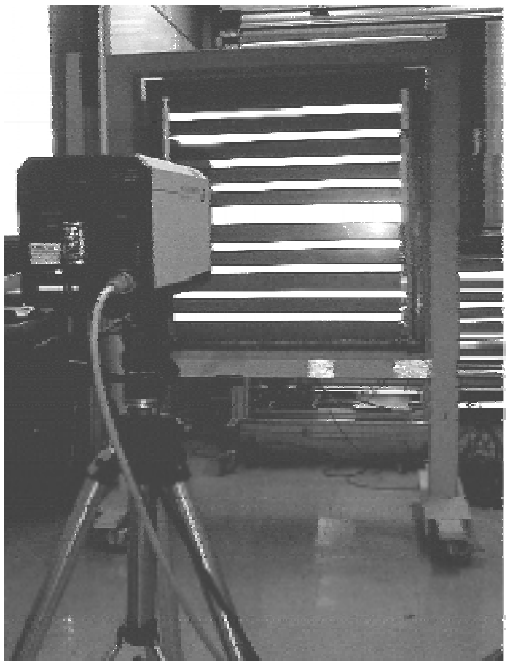

Fig. 3. Experimental set-up for measuring the vibrating velocity in the plate using scanning laser vibrometry technique.

4. Techniques of wavenumber processing

As described in the second section, though the STF is an efficient and fast tool to compute any order partial derivatives of the velocity, the operation of SFT amplifies the components of high wavenumber, causing large contributions of the high wavenumber components to the results. This distortion is even large in the case of the higher-order partial derivatives of the velocity. In addition, when SFT applies to a truncated signal, a distortion is that no existing high frequency components are created. Furthermore the processing of the hologram field must be finite and discrete because data acquisition is done on a finite-size hologram. This finite aperture restriction leads to an error of wraparound on the wavenumber spectrum. This section focuses on the techniques of wavenumber processing to reduce the distortions in using SFT directly. A new technique called mirror method is introduced. Comparisons among direct SFT, zero padding and mirror method used are made through examples of calculating derivatives.

Zero padding method is often used to reduce the wraparound error. In this method surrounding the plate size ($L_x \times L_y$), respectively length and width of the plate) a band of zero is added, forming a $2L_x \times 2L_y$ aperture in which the SFT is applied [20]. This procedure gives good results when the plate is simply-supported or clamped. In these cases "zero padding"

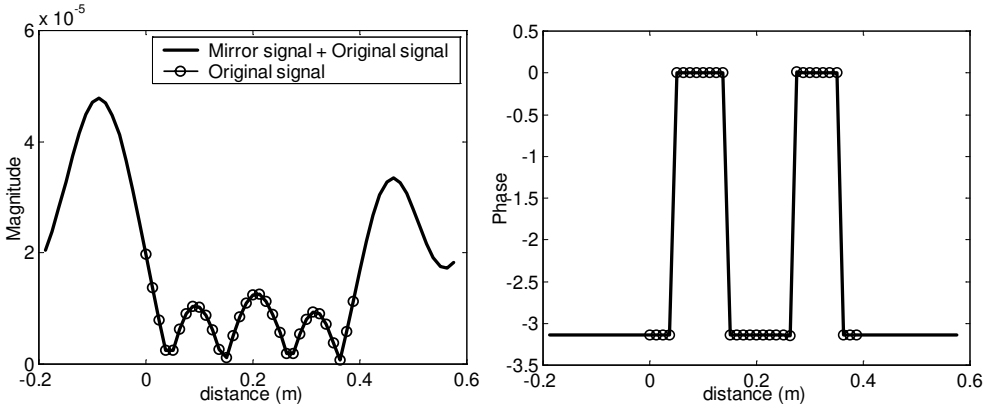

Fig. 4. Magnitude (left) and phase (right) of the complex-displacement signal $v(x)$ of a beam with free-free boundary excited by a harmonic point force. The calculation frequency is 500 Hz. The continuous and periodic displacement signal (solid line) is built from the original displacement signal (o-o-o-o) using a cosine link function.

method can be used to solve the distortion problems encountered with the odd vibrational modes. However this method falls for other boundary conditions where the vibrating velocity is not zero at the edges of the plate. A plate with free-free boundary conditions is one of cases to be hardly treated. In order to solve this problem, a new technique called mirror method is developed.

The idea of the mirror method is to build a continuous and periodic signal (the resulting signal) from the signal to be processed by SFT (the original signal). In this method, the original image is mirrored with respect to its ends, (for a plate, they correspond to the edges of the plate) using a "link function". The resulting signal that is continuous and periodic is the addition of the original image to the mirrored image so that it has approximately double size of the original signal. As the SFT is applied to the resulting signal, the leakage effects are removed. Good estimations for the higher-order partial derivatives of the signal can be obtained as it can be shown in the following examples.

Let S be an original signal with a dimension $[M \times N]$. R is the image signal of S and is of a dimension $[M-2, N-2]$. The resulting signal S_m is built by connecting the two equal parts of the image signal R respectively with the left and right ends of the original signal S. So the dimension of S_m is of $[2M-2, 2N-2]$. The difficulty to build S_m is to solve the step phenomenon at the two connection ends. Therefore choosing a "link function" is a key to the mirror method. A good "link function" should guarantee the periodic-continuity condition for the resulting signal. As an example, we work on one-dimensional vector of M elements $[1, M]$ to show how the "link functions" work to make the image signal smoothly connecting with the left and right ends of the original signal.

– *Linear link function:* It is a simplest form for re-building the image signal. The image signal is the linear reflection of the original signal.

$$\begin{aligned} &R(r) \\ &= R(r) - 2[S(M) - S(1)]\frac{r}{M-1}, \\ &r = 1, 2, 3, \ldots, (M-2). \end{aligned} \tag{11}$$

The disadvantage of this form, however, is that it does not ensure the continuity of the derivatives of the signal at its two ends. To overcome this difficulty, the following methods are provided.

– *Cosine link function:* The image signal is multiplied by a cosine function before connecting the original signal S,

$$\begin{aligned} R(r) = R(r) - [S(M) - S(1)] \\ \left[1 - \cos\left(\frac{r\pi}{M-1}\right)\right], \\ r = 1, 2, 3, \ldots, (M-2). \end{aligned} \tag{12}$$

As an example, consider a free-free steel beam of a length of 400 mm, width 10 mm and thickness 3 mm. The beam is excited by a harmonic point force at $x_0 = 320$ mm with unit amplitude. The calculation frequency is 500 Hz. The response of the beam to the point force $v(x)$ is calculated by the modal synthesis formulation [21]. Figure 4 shows the resulting signal (mirrored + original signals) using cosine link function. The original signal is also shown in Fig. 4. It is demonstrated that unlike the original signal, the resulting signal is periodic and continuous.

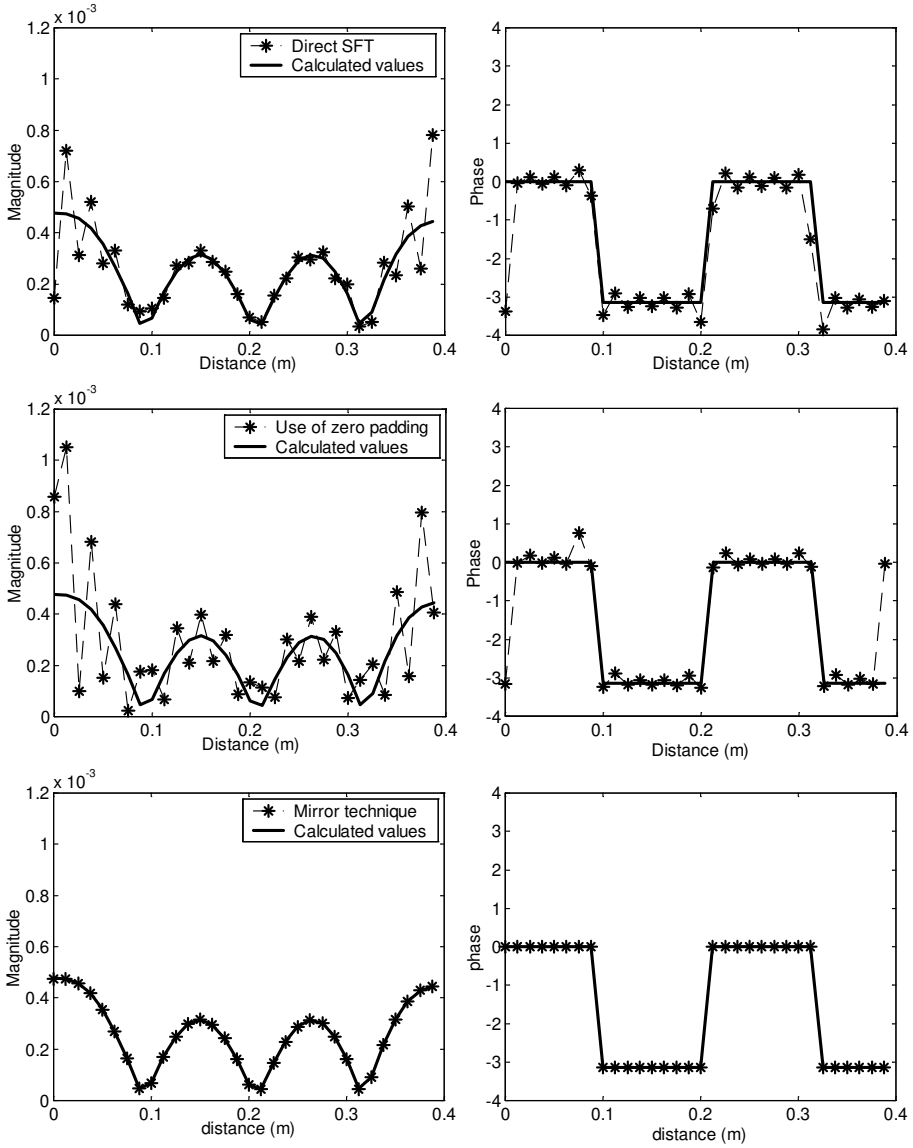

Fig. 5. Magnitude (left) and phase (right) of the derivative of the displacement dv/dx of a beam with free-free boundary conditions excited by a point force at $f = 500$ Hz obtained by processing in wavenumber domain: use of direct SFT (top), use of zero-padding (middle), use of mirror method (bottom). The exact values of dv/dx are represented by the solid line.

To evaluate the performance of the mirror technique, the derivative of the displacement with respect to x is calculated using wavenumber processing. Three methods of calculations are employed to obtain the displacement spectra $V(K_x, K_y)$, which then used to calculate the spectra of the derivative of the displacement using Eq. (7)

a) Perform directly the SFT to the original displacement signal (here the sampling numbers are $M = 32$),
b) Use firstly the zero padding technique (2M elements), then perform the SFT
c) Build a new signal using mirror technique (2M-2 elements), then the SFT is performed to the new signal.

The spatial derivative dv/dx (it could be real or complex) is obtained by performing the inverse Fourier transform to the spectrum of derivative. Figure 5 shows the results of the three methods. The exact values are also shown in Fig. 5 for comparisons. It is noted that the results of the calculations of dv/dx using the direct

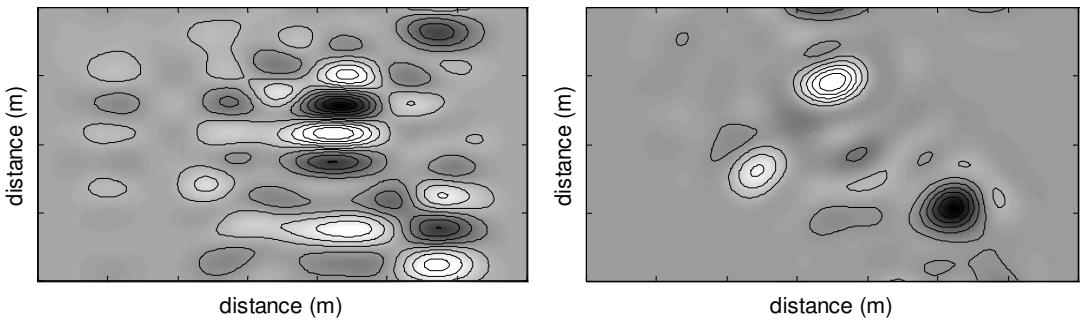

Fig. 6. Divergence of the structural intensity for a plate with free-free boundary conditions obtained by processing the measured vibrating normal velocity in wavenumber domain using respectively direct SFT (left) and the mirror method (right) before the Fourier transform is performed. The divergence is represented by gray scales. The representation dynamic is 20 dB.

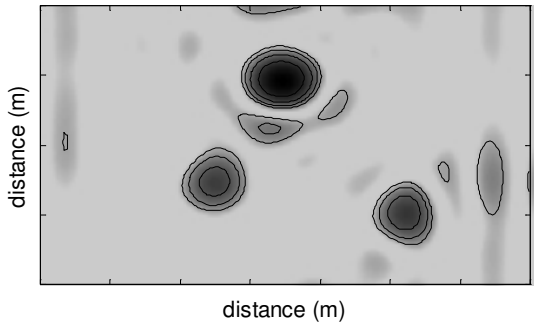

Fig. 7. Force distributions in the plate evaluated by processing vibrating velocity in wavenumber domain with mirror method being used. The square of force amplitudes is represented by gray scales.

SFT and zero-padding method are different from those of the exact results especially at the ends of the beam. Good agreements are found between the derivative obtained by using the mirror technique with cosine link function and the exact values of the derivative dv/dx.

5. Use of mirror techniques in experimental data processing

The objective of this section is to show the use of the techniques of wavenumber processing developed in the previous sections. The complex velocity $v(x, y)$ of a brass plate with free-free boundary was measured on a mesh grid of 32 by 32 using the technique of scanning laser vibrometry shown in Fig. 3. The dimension of the brass plate is 350 mm $\times$ 200 mm $\times$ 3 mm. The excitation frequency is 1160 Hz. The processing algorithm employed in wavenumber domain to calculate the structural intensity and its divergence from the knowledge of the vibrating velocity on the plate $v(x, y)$ is implemented as follows:

1) Input the vibrating velocity data $v(x, y)$ and plate geometry and mechanics parameters.
2) Build mirrored velocity data file $v_m(x, y)$ using mirror technique described in Section 4.
3) Perform the discrete Fourier transform of $v_m(x, y)$ and called it $V(K_x, K_y)$.
4) Apply k-space window to the velocity spectra and obtain the windowed spectra $V(K_x, K_y)W(K_x, K_y)$ to remove the noise-contaminated components at high frequencies. There exist several K-space windows [22], one of which is given by

$$W(K_x, K_y) = \begin{cases} 1, & \text{for } K_r = 0; \\ 1 - 0.5\exp[-(K_c/K_r - 1)/s], & \\ \quad \text{for } K_r \leqslant K_c & \\ 0.5\exp[(1 - K_r/K_c)/s], & \\ \quad \text{for } K_r \geqslant K_c & \end{cases} \tag{13}$$

where $K_r = \sqrt{K_x^2 + K_y^2}$, K_c is the cut-off wavenumber, s is the window shape parameter and is taken as $s = 0.1$. Good results are obtained when K_c is chosen to conserve 90% to 98% of the vibrational kinetic energy of the measurement data.
5) Calculate the spectra of one- to four-order derivatives of the velocity with respect to the coordinates (x, y) in wavenumber domain by the use of Eq. (7). Then compute the inverse Fourier transform of each of the spectra to obtain the derivatives in real space.
6) Use Eqs (8), (9) and (10) to calculate respectively the near-field structural intensities, the divergence and the force distributions.

The divergence of the structural intensity was calculated by Eq. (9) using measured vibrating velocity.

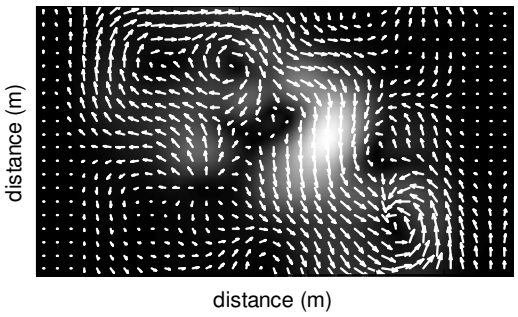

Fig. 8. Structural intensities of a plate with free-free boundary conditions obtained by processing the measured vibrating normal velocity in wavenumber domain with mirror method being used. The in-plane components (I_x, I_y) of the structural intensity are represented graphically by arrows. The amplitude of the structural intensity $\sqrt{I_x^2 + I_y^2}$ is represented by the grey scales. The representation dynamic is 20 dB.

Direct FFT and mirror method were respectively used. Results are illustrated in Fig. 6. It is noted that the excitation position on the plate cannot be located if the Fourier transform was directly performed to the measured vibrating velocity (see Fig. 6 left). Whereas if the velocity spectra $V(K_x, K_y)$ is estimated by the mirror technique, the positions of the excitation (two white spots) and damping (black spot) areas on the plate are clearly located as seen in Fig. 6 (right).

Excitation force distributions in the plate given by Eq. (10) were calculated by processing in wavenumber domain with mirror method being used. Square of amplitudes of forces is shown in Fig. 7. It is demonstrated that the three-excitation forces are well located. In Fig. 8 is shown the structural intensities of the plate with free-free boundary conditions at 1160 Hz. K-space window with cut-off wavenumber 150 rad/m is applied in all calculations. Energy flow in the plate can be observed from the map of the structural intensity. It is also noted that only two excitation forces can be localized from this map: the first one from which the intensity vectors are divergent and the second to which the intensity vectors are convergent. The third excitation force cannot be located by the intensity map because of vortices. However the use of the divergence map allows the third force to be located.

6. Conclusion

Optical techniques such as the holographic interferometry and laser vibrometry, can be used to obtain the map of normal component of the complex vibrating velocity on a plate. The velocity is then processed to compute the structural intensity, the divergence of the structural intensity and the force distributions. The technique of processing in wavenumber domain is based on the Spatial Fourier transform. It is a very efficient method for evaluations of the spatial derivatives used in calculation of the structural intensity and divergence of intensity. However leakage effects are not avoidable if direct use of the Fourier transform is made. A technique – mirror method – is developed and demonstrated to overcome this problem. A noticeable improvement on the quality of the spectrum can be obtained by the use of the mirror method. As a result, the higher-order partial derivatives required in the computations of the structural intensity and the divergence in a plate are estimated precisely. Excitation and damping areas are located from the map of the divergence of the structural intensity in a plate with free-free boundary conditions.

Acknowledgments

This work was done within the framework of the Brite Euram VIP project BE96-3192.

References

[1] Proceedings of the 4th International Congress on Intensity Techniques, Senlis, France, 31 August–2 September, 1993.
[2] J.C. Pascal, T. Loyau and J.A. Mann III, Structural Intensity from spatial Fourier transformation and BAHIM acoustical holography method, *Proc. Cong. On Structural Intensity and Vibrational Energy Flow,* Senlis, France, 27–29 Aug. 1990, pp. 197–204.
[3] Noiseux, Measurement of power flow in uniform beams and plates, *J. Acoust. Soc. Am.* **47**(1) (1970), 238–247.
[4] G. Pavic, Measurement of structure borne wave intensity, Part I: Formulation of the methods, *J. Sound. Vib.* **49**(2) (1976), 221–230.
[5] J.R.F. Arruda and P. Mas, Predicting and measuring flexural power flow in plates, *2nd Int. Conf. On Vibration Measurement by Laser Techniques,* SPIE Vol. 2868, Ancona, Italy, 23–25 September 1996, pp. 149–163.
[6] J.M. Cuschieri, Experimental measurement of structural intensity on an aircraft fuselage, *Noise Control Eng.* **37**(3) (1991), 97–107.
[7] E.G. Williams, H.D. Dardy and R.G. Fink, Technique for measurement on structure borne intensity in plates, *J. Acoust. Soc. Am.* **78**(6) (1985), 2061–2068.
[8] J.C. Pascal, T. Loyau and X. Carniel, Complete determination of structural intensity in plates using laser vibrometers, *J. Sound Vib.* **161**(3) (1993), 527–531.
[9] J.D. Blotter, D.H. Coe, R.L. West and L.D. Mitchell, New developments in experimental spatial power flow, *Proc. of Inter-Noise 96,* Liverpool, UK, 31 July–2 August, 1996, pp. 1423–1428.

[10] J.C. Pascal, X. Carniel, V. Chalvidan and P. Smigielski, Determination of structural intensity and mechanical excitation using holographic interferometry, *Proc. Cong. On Structural Intensity and Vibrational Energy Flow,* Senlis, France, 31 Aug.–2 Sept. 1993, pp. 137–144.

[11] J.C. Pascal, X. Carniel, V. Chalvidan and P. Smigielski, Determination of phase and amplitude of vibration for energy flow measurements in a plate using holographic interferometry, *Optics and Lasers in Engineering* **24** (1996), 1–18.

[12] P. Smigielski, V. Chalvidan, P. Albe, J.C. Pascal and X. Carniel, Double-exposure holographic cinematography for in-situ vibration analysis, *Proc. SPIE's International Symposium on Optical Science, Engineering and Instrumentation,* San Diego, USA, 9–14 July, 1995, pp. 1–11.

[13] J.R.F. Arruda, Surface smoothing and partial spatial derivatives computation using a regressive discrete Fourier series, *Mechanical system and signal processing* **6**(1) (1992), 41–50.

[14] Y. Zhang and J.A. Mann III, Measuring the structural intensity and force distribution in plates, *J. Acoust. Soc. Am.* **99**(1) (1996), 345–353.

[15] H. Sander, On the importance of boundary layers for intensity measurements in beams, *Proc. Cong. On Structural Intensity and Vibrational Energy Flow,* Senlis, France, 31 Aug.–2 Sept. 1993, pp. 207–214.

[16] L. Cremer, M. Heckl and E.E. Ungar, *Structure-Borne Sound,* (Second ed., Ch. II), Springer-Verlag, 1988.

[17] M.C. McGary, Simulated measurement of power flow in structures near to simple sources and simple boundaries, *NASA Technical Memorandum 89124,* Langley Research Center, Hampton, USA, 1988.

[18] X. Carniel and L. Gavric, Etude des formulations de l'intensité vibratoire pour les poutres en flexion, *Proc. Cong. On Structural Intensity and Vibrational Energy Flow,* Senlis, France, 27–29 Aug. 1990, pp. 323–330.

[19] G. Pedrini, H. Tiziani and Y. Zou, Digital double pulse TV-holography, *Optics and Laser Engineering* **26** (1997), 199–219.

[20] J.D. Maynard, E.G. Williams and Y. Lee, Nearfield acoustical holography (NAH) I. Theory of generalized holography and the development of NAH, *J. Acoust. Soc. Am.* **78** (1985), 1395–1413.

[21] D.J. Inman, *Engineering vibration,* Prentice Hall, Englewood Cliffs, New Jersey, 1996.

[22] J.F. Li, J.C. Pascal and C. Carles, A new K-space optimal filter for acoustics holography, *Proc. of Third International Congress on Air- and Structure Borne Sound and Vibration,* Monréal, Canada, 13–15 June 1994, pp. 1059–1066.

[23] X. Carniel, J.P. Chambard, J.C. Pascal and P. Monnier, Determination of structural intensity field by pulsed TV-holography at 25 Hz, *Colloque Nouveaux moyens optiques pour l'industrie II,* (Société Française d'Optique), Mittelwihr, 17–19 November 1999, pp. 67–75.